[1]H. L. Ravn, L. C. Carraz, J. Denimal, E. Kugler, M. Skarestad, S. Sundell, and L. Westgaard, Nucl. Instrum. Methods 139, 276 (1976).
[2]P. Dabkiewicz, F. Buchinger, H. Fischer, H.-J. Kluge, H. Kremmling, T. Kuehl, A. C. Mueller, and H. A. Schuessler, Phys. Lett. 82B, 199 (1979).
[3]For a review on quantum beats see S. Haroche, *Topics in Applied Physics* (Springer, Berlin, Hamburg, and New York, 1976), Vol. 13.
[4]G. Breit, Rev. Mod. Phys. 5, 91 (1933).
[5]A. Lurio, Phys. Rev. 140, A1505 (1965).
[6]R. Kalish, R. R. Borchers, and H. W. Kugel, Nucl. Phys. A147, 161 (1971).
[7]A. Bockisch, K. Bharuth-Ram, A. M. Kleinfield, and K. P. Lieb, Z. Phys. A 289, 231 (1979).
[8]D. Proetel, R. M. Diamond, and F. S. Stephens, Phys. Lett. 48B, 102 (1974).
[9]N. Rud *et al.*, Phys. Rev. Lett. 31, 1421 (1973).
[10]F. S. Stephens, Rev. Mod. Phys. 47, 43 (1975).
[11]D. Proetel, D. Benson, A. Gizon, J. Gizon, M. R. Maier, R. M. Diamond, and F. S. Stephens, Nucl. Phys. A226, 237 (1974).
[12]H. H. Stroke, D. Proetel, and H.-J. Kluge, Phys. Lett. 82B, 204 (1979).

Rate Theory for the Four-Photon Ionization of Cs near the 6*F* Resonance

Burke Ritchie
Department of Chemistry, University of Alabama, University, Alabama 35486
(Received 11 May 1979)

A previously presented narrow-bandwidth theory is used to interpret recent data on the four-photon ionization of Cs near the 6*F* resonance. The theory is based on treating the amplitude of the radiation field as a constant relative to its rapid phase oscillations. The ionization rate adiabatically follows a pulsed amplitude leading to maximum ionization for times at which the pulse develops sufficient intensity to shift the $6S \rightarrow 6F$ transition into resonance.

In a previous paper[1] (I) a formalism was presented based on treating the amplitude of the classical radiation field $b(t)$, which is slowly varying in the time, as a constant relative to the oscillatory part of the field, which is rapidly varying in the time. Using this adiabatic approximation, the Fourier integral of the field $A(t)$ is proportional to a δ function in frequency space,

$$a(\omega) = (2\pi)^{-1} \int_{-\infty}^{\infty} dt e^{i\omega t} A(t) \simeq b(t)\,\delta(\omega - \omega_p), \quad (1)$$

where ω_p is the constant photon frequency and only the absorptive component of the field is considered. Thus the field depends on $b(t)$ *parametrically*. This form illustrates the single-mode character expected for a very-narrow-bandwidth field such as that of the recent experiment by Morellec and co-workers[2] (II), where the bandwidth is about 2×10^{-3} cm^{-1}.

In the experiment of II the flux F depends on the time. This time dependence is described by multiplying F by a dimensionless Gaussian shape function $G(t)$, with a 37 ns width at half maximum, which generates a maximum F corresponding to an intensity of 10^9 W cm^{-2} at the center of the pulse t_0. It is the purpose of the present paper to evaluate the slowly varying field amplitude $b(t)$, proportional to $[G(t)F]^{1/2}$, as adiabatically following the rapidly varying oscillatory part whose use in the dynamical problem has led to a rate. That is, we replace $b(t)$ in Eq. (1) by $[2\pi G(t)F/\alpha\omega_p]^{1/2}e$. This quantity occurs as a parameter in the time-independent rate. The success of the present adiabatic-following approximation in describing the time dependence of the ionization yield data of II will be demonstrated below and illustrates how a time-independent rate theory[1,3-6] can be used to describe temporal phenomena in laser-induced ionization.

The flux also depends on the focal volume (Figs. 3 and 11 of II). This dependence is given by multiplying the maximum flux (corresponding to an intensity of 10^9 W cm^{-2}) developed at t_0 by a dimensionless shape function $F_S(x, y, z)$, where this function is normalized to 1 at the center of the focal volume, or $F_S(0, 0, 0) = 1$ (Appendix of II). In this paper we multiply $G(t)F$ above by $F_S(0, 0, z)$, where $G(t)$ and $F_S(0, 0, z)$ are constructed from the information given in II [Figs. 11(a), 11(b), and 14]. Our rate[1,3-6] $R_4(z, t)$ for the four-photon ionization of Cs near the 6*F* resonance, for a given time t in the development of the pulse along a path z through the center of the focal volume,

© 1979 The American Physical Society

is

$$R_4(z,t)=\frac{\frac{1}{4}\Omega_3^2(z,t)R_{6F}(z,t)}{[\delta-\Delta(z,t)]^2+[R_{6F}(z,t)/2]^2}, \tag{2a}$$

$$\tfrac{1}{2}\Omega_3(z,t)=\frac{[2\pi F(z,t)\alpha a_0^2]^{3/2}}{(\omega_p)^{1/2}E}\,|\langle\psi_{6F}|\hat{\rho}\cdot\nabla|\chi_2\rangle|, \tag{2b}$$

$$\Delta(z,t)=-\frac{4\pi F(z,t)\alpha a_0^2}{E}\,\mathrm{Re}\sum_{n=2}^{4}{}'[\int\int d^3r\,d^3r'\,\psi_{6F}^*(\vec{r})(\hat{\rho}\cdot\nabla)g^{(M)}(\vec{r},\vec{r}';2(E_{6S}+nE))(\hat{\rho}\cdot\nabla')\psi_{6F}(\vec{r}')], \tag{2c}$$

$$R_{6F}(z,t)=-\frac{8\pi F(z,t)\alpha a_0^2}{E}\,\mathrm{Im}\int\int d^3r\,d^3r'\,\psi_{6F}^*(\vec{r})(\hat{\rho}\cdot\nabla)g^{(M)}(\vec{r},\vec{r}';2(E_{6S}+4E))(\hat{\rho}\cdot\nabla')\psi_{6F}(\vec{r}'), \tag{2d}$$

$$\delta=(\omega_{6S}-\omega_{6F})+3\omega_p. \tag{2e}$$

Where the ω_j's are the atomic eigenfrequencies in s^{-1} (corresponding to the E_j's in atomic units), E is the photon energy in atomic units (for ω_p in s^{-1}), $\hat{p}$ is the unit vector in the direction of polarization of the photon, $F(z,t)=G(t)F_S(0,0,z)F$, and the prime on the sum means that $n=3$ is omitted by parity conservation. The parameters of Eqs. (2) are displayed in Table I. These have been calculated using numerical Hartree-Fock functions.[7] The atomic field Green's functions $g^{(M)}$ are calculated explicitly for energies nE above the ionization continuum ($n=4$) with use of

$$g^{(M)}=(4\pi)^{-1}\textstyle\sum_l(2l+1)g_l^{(M)}(r,r';2(E_{6S}+4E))P_l(\hat{r}\cdot\hat{r}'), \tag{3a}$$

$$g_l^{(M)}=-\frac{1}{krr'}[G_l^{(M)}(kr_>)F_l^{(M)}(kr_<)+iF_l^{(M)}(kr)F_l^{(M)}(kr')], \tag{3b}$$

and by numerical solution for the regular and irregular waves $F_l^{(M)}$ and $G_l^{(M)}$, respectively, in an effective atomic field V (the static potential plus the semiclassical local exchange potential[8] appropriate for Cs^+). For energies nE below the ionization continuum ($n=2$) $g^{(M)}$ is found by defining the function

$$\chi_2^{(M)}(\vec{r})=\int d^3r'\,g^{(M)}(\vec{r},\vec{r}';2(E_{6S}+2E))2(\hat{\rho}\cdot\nabla')\psi_{6F}(\vec{r}') \tag{4}$$

which obeys the differential equation,

$$[\nabla^2-U(r)+2(E_{6S}+2E)]\,\chi_2^{(M)}(\vec{r})=2\hat{\rho}\cdot\nabla\psi_{6F}(\vec{r}), \tag{5}$$

where $U=(2m_e/\hbar^2)V$. χ_2 [see Eq. (2b) above] is the second-order perturbative function of the 6S state. It is calculated from an equation obtained from Eq. (5) by replacing ψ_{6F} by χ_1, the first-order perturbative function of the 6S state. χ_1 is calculated from an equation obtained from Eq. (5) by replacing ψ_{6F} by ψ_{6S} and $2E$ by E. The radial equations derived from these equations are solved numerically.

TABLE I. Atomic parameters in units of frequency, $\omega(\omega/2\pi=c/\lambda)$, at an intensity of 10^9 W cm^{-2} or $F=0.5335\times10^{28}$ cm^{-2} s^{-1} at $\dot{o}=0$ s^{-1}.

This work[a]	Experiment[b]
$\Omega_3=1.735\times10^9$ s^{-1}	
$R_{6F}=1.569\times10^{10}$ s^{-1}	
$\Delta=2.767\times10^{11}$ s^{-1}	$\Delta=4.308\times10^{11}$ s^{-1}
$\sigma_{6F}^{(V)}=R_{6F}/F=2.942\times10^{-18}$ cm^2	
$\sigma_{6F}^{(L)}=2.720\times10^{-18}$ cm^2	

[a]The superscripts on the photoelectric cross sections designate velocity (V) and length (L) forms.

[b]See Table I of II, based on a measured shift of 0.8 cm^{-1} for an intensity of 0.35×10^9 W cm^{-2}.

The rate $R_4(z,t)$ of Eq. (2a) is in agreement with that of Eberly and co-workers[4,5] at high power levels or when $\frac{1}{4}R_{6F}^2\gg\frac{1}{2}\Omega_3^2$ (see Table I) and when R_{6F} is dominant over A and W, the Einstein spontaneous decay width and laser bandwidth, respectively. It is also in agreement with the rate calculated by Crance[9] when the nonresonant background is ignored close to resonance. When we find $\ln R_4(z,t)$ and take its derivative with respect to $\ln F(z,t)$ (the order of nonlinearity), we find agreement with Eberly[6] in this same high-power limit,

$$K^{(4)}=4-\frac{2[\Delta^2+(\frac{1}{2}R_{6F})^2-\delta\Delta]}{[(\delta-\Delta)^2+(\frac{1}{2}R_{6F})^2]}. \tag{6}$$

In Fig. 1 this result is plotted at the centers of the Gaussian pulse and of the focal volume [for $G(t_0)F_S(0,0,0)=1$] for the atomic parameters given in Table I. The shift is located at the point $\delta=\Delta=1.469$ cm^{-1} (see Table I for Δ), where $K^{(4)}$

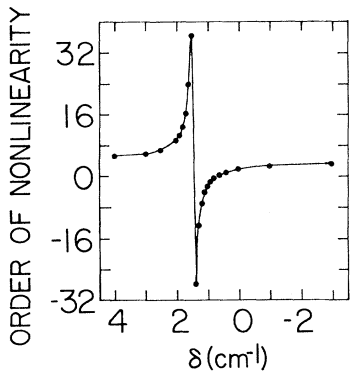

FIG. 1. Order of nonlinearity for the parameters shown in Table I using Eq. (6) at t_0 and $x=y=z=0$ (center of the Gaussian pulse and center of the focal volume, respectively).

passes steeply through 2.

$R_4(z,t)$ is plotted in Fig. 2 for an $F(z,t)$ distribution corresponding to an intensity distribution shown in Fig. 3 and $\delta = 1.35$ cm^{-1}. δ (equal to $-\Delta_0$ of II) is chosen to approximately yield a maximum ionization rate, produced by "dynamic compensation"[2] at $\delta = \Delta$, obtained for an intensity near $t_0 - 8$ ns rather than at t_0, where a maximum intensity of 10^9 W cm^{-2} occurs at $z = 0$. That dynamic compensation is not precisely reached at $t_0 - 8$ ns is reflected in the small splitting of the peak at $z = 0$. The t_0 minimum at $z = 0$ (where the full 10^9 W cm^{-2} intensity is developed) illustrates that dynamic overcompensation has occurred (the $6F$ level has been repelled out of resonance at this power level). Figure 3 should be compared with Fig. 11(b) of II along z, where the origin ($z = 0$) at the center of the focal volume is located at the center of the intensity distribution in the latter figure (point of the largest peak) Figure 2 should be compared with Figs. 11(e) and 11(f) of II along z, where in the latter figures the center of the focal volume is located at the center of the N_i distribution. The behavior shown in Fig. 2 is in qualitative agreement with the experimental space-time behavior of the ionization rate near resonance.

We obtain an ionization probability for any point along z, the path of the beam through the center of the focal volume (Fig. 3 of II), by integrating the rate over the time,

$$P_i(z) = \int_0^\infty dt\, R_4(z,t) \exp\left(-\int_0^t dt'\, R_4(z,t')\right), \quad (7)$$

where the exponential factor gives the probability of finding an unionized atom along z at t. We define an order of nonlinearity K_{expt} along z by numerically taking the derivative of $\ln P_i(z)$ with respect to $\ln F(z,t)$ in the limit as $t \to \infty$. These results are plotted in Fig. 4 for the values of z shown. Also plotted is the order of nonlinearity averaged over z by integrating K_{expt} over z and dividing the result by the interval of integration, -10 mm $\leq z \leq +10$ mm. Figure 4 should be compared with Fig. 7 of II. However, the experimental K_{expt} (Appendix of II) is an average value

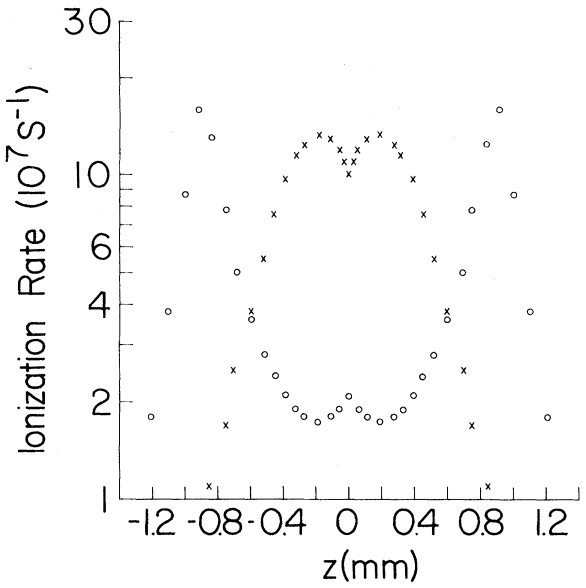

FIG. 2. Ionization rate $[R_4(z,t)]$ for the times shown along a path in the beam direction running through the center of the focal volume ($x=y=z=0$). Circles, at t_0; crosses, at $t_0 - 8$ ns.

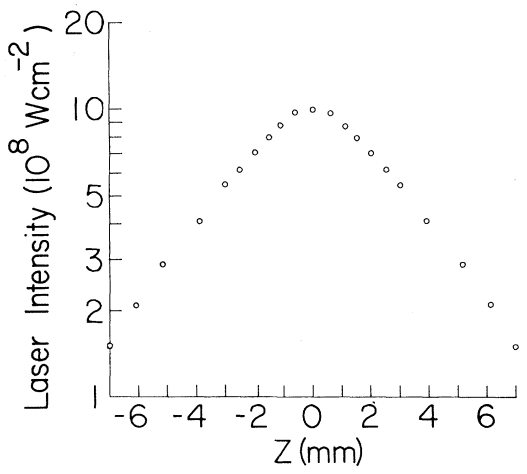

FIG. 3. Laser intensity distribution at t_0 (center of the Gaussian pulse) along a path in the beam direction running through the center of the focal volume ($x=y=z=0$).

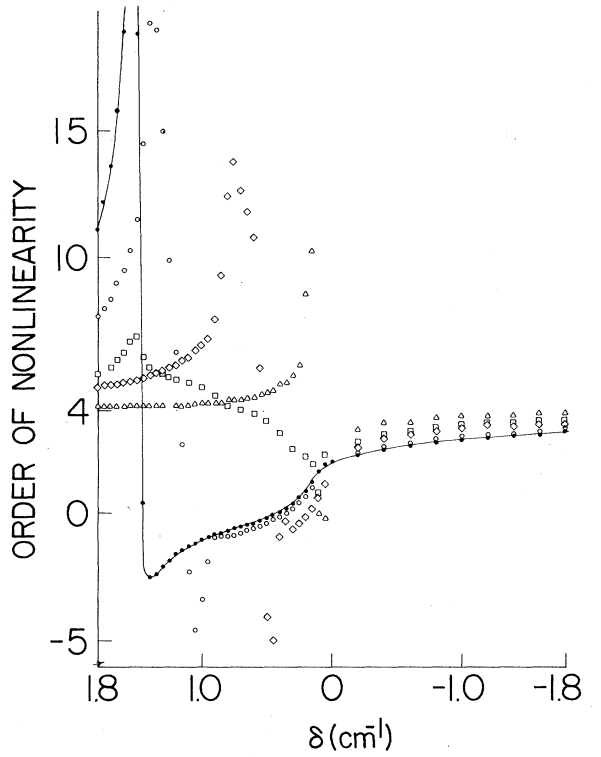

FIG. 4. Order of nonlinearity based on the derivative of $\ln P_i(z)$ [Eq. (7)] with respect to $\ln F(z,t)$ at large times when the Gaussian pulse is sufficiently damped that there are no further contributions to $P_i(z)$. Solid circles: $z=0.034$ mm; open circles: $z=1.27$ mm; diamonds: $z=3.86$ mm; triangles: $z=8.18$ mm; squares: results averaged along z.

in the entire focal volume, requiring the construction of a flux surface $G(t)F_S(x,y,z)F$ and the calculation of an ionization probability surface $P_i(x, y, z)$. Although a precise comparison cannot be made for this reason, we note that our average order of nonlinearity for values $\delta \leq 0$ tends to show better agreement with the data than our Fig. 1 or Fig. 2 of Ref. 6, where the latter are calculated at a single flux. Although the measured K_{expt} needs further theoretical explanation, we are inclined to conclude on the basis of our Fig. 3 that the parametric dependence of the rate on a flux time surface $F_S(x, y, z, t)$ and the calculation of the ionization probability in an adiabatic-following approximation would provide a physically correct description of the space-time behavior of the ionization process studied in II. Thus we are inclined to agree with Eberly and co-workers[4-6] that the data represent a "smoothed time-integrated signal"[4] in which the temporal features of the dynamical process do not occur; thus a time-independent rate theory[1,3-6] can be used to interpret such data. On the other hand, we are inclined to disagree with the conclusion of Gontier and Trahin[10] on the interpretation of the same data that "the notion of a time-independent rate can be seen to be inadequate."

[1]B. Ritchie, Phys. Rev. A 17, 659 (1978).
[2]J. Morellec, D. Normand, and G. Petite, Phys. Rev. A 14, 300 (1976); also see G. Petite, J. Morellec, and D. Normand, J. Phys. (Paris) 40, 115 (1979).
[3]B. Ritchie, Phys. Rev. A (to be published).
[4]J. L. F. de Meijere and J. H. Eberly, Phys. Rev. A 17, 1416 (1978).
[5]J. H. Eberly and S. V. O'Neil, Phys. Rev. A 19, 1161 (1979).
[6]J. H. Eberly, Phys. Rev. Lett. 42, 1049 (1979).
[7]C. Froese, Phys. Rev. 45, 1417 (1966). The excited states are calculated in the field of Cs^+. All level energies are taken from C. E. Moore, *Atomic Energy Levels as Derived from Analyses of Optical Spectra*, National Bureau of Standards Circular No. 467 (U. S. GPO, Washington, D. C. 1949), Vol. I.
[8]M. E. Riley and D. G. Truhlar, J. Chem. Phys. 63, 2182 (1975).
[9]M. Crance, J. Phys. B 11, 1931 (1978).
[10]Y. Gontier and M. Trahin, Phys. Rev. A 19, 264 (1979).